

Preparation of Monodispersed Fe–Mo Nanoparticles as the Catalyst for CVD Synthesis of Carbon Nanotubes

Yan Li and Jie Liu*

Department of Chemistry, Box 90346, Duke University, Durham, North Carolina 27708

Yongqian Wang and Zhong Lin Wang

School of Materials Science and Engineering, Georgia Institute of Technology,
771 Ferst Drive, N.W., Atlanta, Georgia 30332

Received September 29, 2000. Revised Manuscript Received December 19, 2000

Uniform iron–molybdenum nanoparticles were prepared by thermal decomposition of metal carbonyl complexes using a mixture of long-chain carboxylic acid and long-chain amine as protective agents. The sizes of the nanoparticles can be systematically varied from 3 to 14 nm by changing the experimental conditions. High-resolution TEM images and EDX data show that the prepared nanoparticles are highly crystalline iron nanoparticles containing $\approx 4\%$ molybdenum. The effects of the concentration, reaction time, the ratio of metal carbonyl complexes versus protective agents, and the ratio of acid/amine of the protective agents on the sizes of the produced nanoparticles were systematically studied. The prepared nanoparticles were used as catalysts for single-walled carbon nanotube growth and the results indicate that there is an upper limit for the size of the catalyst particles to nucleate single-walled carbon nanotubes.

Introduction

Metal nanoparticles have been attracting intensive interest because of their outstanding properties and potential applications in the areas of catalysis,¹ magnetism,² electronics,³ and so forth. They have been fabricated by using various chemical or physical methods.⁴ However, because many properties of these nanoparticles are size-dependent, how to obtain uniform nanoparticles becomes one of the key problems in the area of nanoscience and technology.⁵ Significant efforts have long been concentrated on the precise control of the particles' size distribution.⁶ To date, the chemical

pathways carried out in solution have been very successful in obtaining nanoparticles with narrow size distributions.^{7–10} Normally, the metal nanoparticles were prepared either in microreactors formed by surfactant molecules (such as in micelles)⁸ or in solutions of polymers⁹ or other coordinating reagents that bind to the surface of the nanoparticles and prevent them from growing bigger.¹⁰ This way, the size and size distribution of the particles can be controlled to some extent. However, the precise control of the particle size is still a challenge.

Because of their interesting magnetic properties, pure iron and iron alloy nanoparticles have been widely studied.^{11–15} Fe nanoparticles are normally obtained by the reduction of iron salts in micelles¹¹ or by thermal^{12,13} or sonocative¹⁴ decomposition of iron pentacarbonyl in solutions with certain polymers as protective agents. The alloy particles were prepared in similar ways. But

* To whom correspondence should be addressed. E-mail: jliu@chem.duke.edu.

(1) (a) Pathak, S.; Greci, M. T.; Kwong, R. C.; Mercado, K.; Prakash, G. K. S.; Olah, G. A.; Thompson, M. E. *Chem. Mater.* **2000**, *12*, 1985. (b) Zhao, M.; Crooks, R. M. *Adv. Mater.* **1999**, *11*, 217. (c) Aiken, J. D.; Finke, R. G. *Chem. Mater.* **1999**, *11*, 1035.

(2) (a) Matjetich, S. A.; Jin, Y. *Science* **1999**, *284*, 470. (b) Shi, J.; Babcock, K.; Awschalom, D. D. *Science* **1996**, *271*, 937. (c) Russier, V.; Petit, C.; Legrand, J.; Pileni, M. P. *Phys. Rev. B* **2000**, *62*, 3910.

(3) (a) Andres, R. P.; Bein, T.; Dorogi, M.; Feng, S.; Henderson, J. I.; Kubiak, C. P.; Mahoney, W.; Osifchin, R. G.; Reifengerger, R. *Science* **1996**, *272*, 1323. (b) Petit, C.; Cren, T.; Roditchev, D.; Sacks, W.; Klein, J.; Pileni, M. P. *Adv. Mater.* **1999**, *11*, 1198. (c) Zhang, X. X.; Liu, H.; Fung, K. K.; Qin, B. X. *Physica B* **2000**, *279*, 185.

(4) (a) Ahmadi, T. S.; Wang, Z. L.; Green, T. C.; Henglein, A.; El-Sayed, M. A. *Science* **1996**, *272*, 1924. (b) Andres, R. P.; Bielefeld, J. D.; Henderson, J. I.; Janes, D. B.; Kolagunta, V. R.; Kubiak, C. P.; Mahoney, W. J.; Osifchin, R. G. *Science* **1996**, *273*, 1690. (c) Zach, M. P.; Penner, R. M. *Adv. Mater.* **2000**, *12*, 878.

(5) Rao, C. N. R.; Kulkarni, G. U.; Thomas, P. J.; Edwards, P. P. *Chem. Soc. Rev.* **2000**, *29*, 27.

(6) (a) Watzky, M. A.; Finke, R. G. *J. Am. Chem. Soc.* **1997**, *119*, 1038. (b) Bradley, J. S.; Tesche, B.; Busser, W.; Masse, M.; Reetz, R. T. *J. Am. Chem. Soc.* **2000**, *122*, 4631. (c) Bromann, K.; Félix, C.; Brune, H.; Harbich, W.; Monot, R.; Buttet, J.; Kern, K. *Science* **1996**, *274*, 956. (d) Vidoni, O.; Philippot, K.; Amiens, C.; Chaudret, B.; Balmes, O.; Malm, J. O.; Bovin, J. O.; Senocq, F.; Casanove, M. J. *Angew. Chem., Int. Ed.* **1999**, *38*, 3736.

(7) Schmid, G. *Chem. Rev.* **1992**, *92*, 1709.

(8) (a) Petit, C.; Taleb, A.; Pileni, M. P. *J. Phys. Chem. B* **1999**, *103*, 1805. (b) Taleb, A.; Petit, C.; Pileni, M. P. *Chem. Mater.* **1997**, *9*, 950. (c) Chen, D.-H.; Wu, S.-H. *Chem. Mater.* **2000**, *12*, 1354.

(9) (a) Wang, Y.; Ren, J.; Deng, K.; Gui, L.; Tang, Y. *Chem. Mater.* **2000**, *12*, 1622. (b) Teranishi, T.; Hosoe, M.; Tanaka, T.; Miyake, M. *J. Phys. Chem. B* **1999**, *103*, 3818–3827. (c) Sun, Y. P.; Rollins, H. W.; Guduru, R. *Chem. Mater.* **1999**, *11*, 7.

(10) Reetz, M. T.; Maase, M. *Adv. Mater.* **1999**, *11*, 773.

(11) (a) Wilcoxon, J. P.; Provencio, P. P. *J. Phys. Chem. B* **1999**, *103*, 9809. (b) C. T.; O'Connor, C. J. *Nanostruct. Mater.* **1999**, *12*, 183.

(12) Smith, T. W.; Wychlick, D. *J. Phys. Chem.* **1980**, *84*, 1621.

(13) (a) Griffiths, C. H.; O'Horo, M. P.; Smith, T. W. *J. Appl. Phys.* **1979**, *50*, 7108. (b) van Wenterghem, J.; Morup, S. *Phys. Rev. Lett.* **1985**, *55*, 410.

(14) (a) Suslick, K. S.; Hyeon, T. *J. Am. Chem. Soc.* **1996**, *118*, 11960. (b) Suslick, K. S.; Hyeon, T.; Fang, M. *Chem. Mater.* **1996**, *8*, 2172. (c) Cao, X.; Kolytyn, Y.; Kataby, G.; Prozorov, R.; Gedanken, A. *J. Mater. Res.* **1996**, *79*, 1642.

(15) Sun, S.; Murray, C. B.; Weller, D.; Folks, L.; Moser, A. *Science* **2000**, *287*, 1989.

in most of these works, only multidispersed particles were obtained. Recently, Sun et al.¹⁵ reported the synthesis of monodispersed FePt nanoparticles by the reduction of platinum acetylacetonate and decomposition of iron pentacarbonyl. After size-selecting purification via a two-step “recrystallization”, they got FePt nanoparticles with a standard deviation of <5%.

Although the main interests relating to iron-containing nanoparticles are concentrated on their potential application as high-quality magnetic materials,¹⁶ they also have many other extraordinary properties. For example, iron nanoparticles have been widely used as the catalyst for CVD synthesis of multiwalled carbon nanotubes,¹⁷ and iron–molybdenum can act as a very efficient catalyst for the synthesis of either single-walled or multiwalled carbon nanotubes with the CVD method.^{18–21} It is generally believed that the diameter of the tubes is determined by the size of catalyst particles.²² However, because of the difficulties of making uniform nanoparticles, there have been no systematic studies using preformed uniform catalyst particles. In this paper, we describe the synthesis of monodispersed iron–molybdenum nanoparticles by thermal decomposition of metal carbonyl complexes. This represents the first step in studying the relationship between the size of nanotubes and catalysts and pursuing a systematic investigation of the formation mechanism for carbon nanotubes.

Experimental Section

Materials. Iron pentacarbonyl, molybdenum hexacarbonyl, octanoic acid, bis-2-ethylhexylamine, and octyl ether are all from Aldrich and used as received.

Synthesis of Nanoparticles. Fe–Mo nanoparticles were obtained by the thermal decomposition of their carbonyl complexes in octyl ether solution under a N₂ atmosphere. Octanoic acid and/or bis-2-ethylhexylamine were used as the protective agents to prevent the nanoparticles from aggregating. Typically, 0.196 g of Fe(CO)₅ (1.00 mmol), 0.053 g of Mo(CO)₆ (0.020 mmol), 0.144 g of octanoic acid (0.100 mmol), and 0.242 g of bis-2-ethylhexylamine (0.100 mmol) were dissolved in 5.00 mL of octyl ether and refluxed under a N₂ atmosphere for 30 min. The solution turned black upon the formation of Fe–Mo nanoparticles. 20 mL of propanol was added to precipitate the nanoparticles. The precipitates were re-dispersed in *n*-heptane. The amount of the reactants, the amount of protective agents, and the reaction time were systematically changed in our study to gain control over the sizes of the produced nanoparticles. However, the initial molar ratio between Fe(CO)₅ and Mo(CO)₆ was fixed to 5:1 and the volume of octyl ether was fixed to 5 mL in all our experiments.

The initial concentration of Fe(CO)₅ is 1.0 mmol and the reaction time is 30 min unless otherwise specified.

Characterization. The produced nanoparticles and nanotubes grown from the nanoparticles were characterized with a Philips 301 transition electron microscopy operated at 80 kV. The high-resolution images were obtained using a JEOL 4000EX TEM operated at 400 kV. EDX spectra were collected in Hitachi HF-2000 STEM operated at 200 kV.

Nanotube Growth. The growth of single-walled nanotubes was performed by using a method similar to that in ref 20. The nanoparticles dispersed in *n*-heptane were drop-dried on silicon wafers coated with thin Al₂O₃ films fabricated by the sol–gel method.²⁰ The wafers were then put into a furnace equipped with a quartz tube and gas-flow controllers. They were first reduced in H₂ for 15 min at 900 °C, and then CVD was performed with methane for 30 min at the same temperature. Finally, the system was cooled under an argon atmosphere. The wafers were studied with a Nanoscope IIIA atomic force microscope (Digital Instruments, St. Barbara, CA) operated in tapping mode. Nanoparticles were also dispersed on fumed Al₂O₃ powder (Degussa Corp., Ridgefield Park, NJ) and nanotubes grown on the powder were characterized with TEM.

Results and Discussion

Effect of Protective Agents. The effectiveness of a protective agent in the synthesis of nanoparticles could be evaluated by the size and size distribution of the prepared nanoparticles. Generally speaking, smaller and more uniform nanoparticles indicate that the protective agents interact more strongly with the nanoparticles, forming a more stable protecting layer. However, there are other factors that may also have strong effects on the size and distribution of the prepared nanoparticles as discussed in more detail below.

It is known that carboxylic groups can interact strongly with iron metals. Long-chain carboxylic acids can absorb onto the surface of the metal nanoparticles, forming a dense monolayer and acting as a protective agent. As shown in Figure 1A, when 1.0 mmol of octanoic acid was used as the protective agent, Fe–Mo nanoparticles with ≈11.0 nm diameter was obtained. The diameter distribution of the produced nanoparticles was very narrow, showing that octanoic acid did behave as a protective agent. However, changing the concentration of octanoic acid does not seem to have a strong effect on the produced nanoparticles. Figure 1B shows the nanoparticles made with 2.5 mmol of octanoic acid as the protective agent. The size of the particles is still about 11 nm with a narrow size distribution.

We have also tried to use long-chain amines as the protective agent to make the nanoparticles under similar reaction conditions. Figure 1D,E shows the TEM images of nanoparticles made with bis-2-ethylhexylamine as the protective agent. We found that the size of the produced nanoparticles varies significantly versus the concentration of the amine. The more amine added, the smaller the produced nanoparticles. However, the uniformity of the nanoparticles is much worse than the nanoparticles prepared using octanoic acid as the protective agent and increasing the concentration of amine in the system does not improve the nanoparticles' uniformity. This shows that bis-2-ethylhexylamine has limited protective ability for the formation of Fe/Mo nanoparticles. The reduction in the size of the prepared nanoparticles could be understood as the effect of accelerated decomposition speed of metal carbonyls at higher amine concentration. It was reported that, in

(16) (a) Carpenter, E. E.; Sims, J. A.; Wienmann, J. A.; Zhou, W. L.; O'Connor, C. J. *J. Appl. Phys.* **2000**, *87*, 5615. (b) Zhang, D. J.; Klabunde, K. J.; Sorensen, C. M.; Hadjipanayis, G. C. *Phys. Rev. B* **1998**, *58*, 14167. (c) Roy, S.; Roy, B.; Chakravorty, D. J. *Appl. Phys.* **1996**, *79*, 1642.

(17) (a) Li, W.; Xie, S.; Qian, L.; Chang, B.; Zou, B.; Zhou, W.; Zhao, R.; Wang, G. *Science* **1996**, *274*, 1701. (b) Xie, S.; Chang, B.; Li, W.; Pan, Z.; Sun, L.; Mao, J.; Chen, X.; Qian, L.; Zhou, W. *Adv. Mater.* **1999**, *11*, 1135.

(18) Cassell, A. M.; Raymakers, J. A.; Kong, J.; Dai, H. *J. Phys. Chem. B* **1999**, *103*, 6484–6492.

(19) Su, M.; Zheng, B.; Liu, J. *Chem. Phys. Lett.* **2000**, *322*, 321.

(20) Su, M.; Li, Y.; Maynor, B.; Buldam, A.; Lu, J. P.; Liu, J. *J. Phys. Chem. B* **2000**, *104*, 6505.

(21) (a) Fan, S. S.; Chapline, M. G.; Franklin, N. R.; Tomblor, T. W.; Cassell, A. M.; Dai, H. *J. Science* **1999**, *283*, 512–514. (b) Cheng, H. M.; Li, F.; Su, G.; Pan, H. Y.; He, L. L.; Sun, X.; Dresselhaus, M. S. *Appl. Phys. Lett.* **1998**, *72*, 3282–3284.

(22) Dai, H. J.; Rinzler, A. G.; Nikolaev, P.; Thess, A.; Colbert, D. T.; Smalley, R. E. *Chem. Phys. Lett.* **1996**, *260*, 471–475.

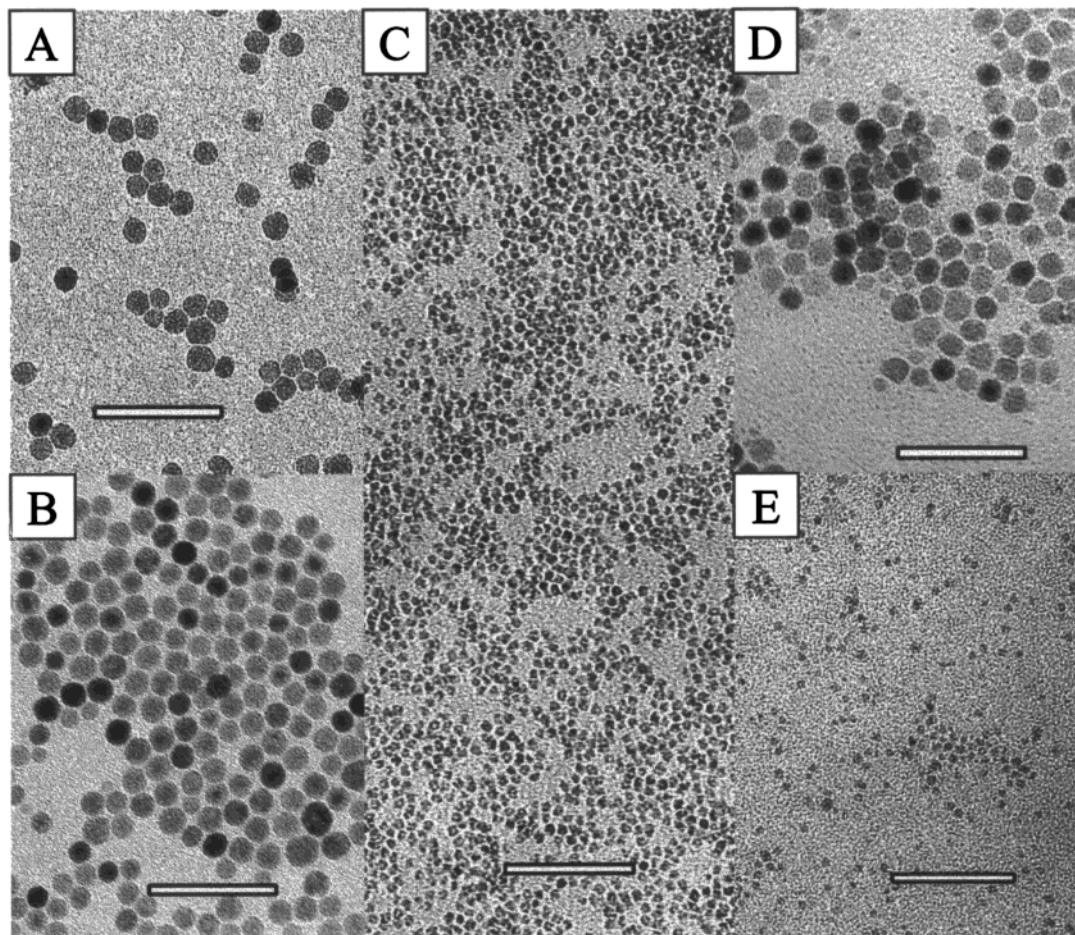


Figure 1. Fe–Mo nanoparticles synthesized with different protective agents. (a) 1 mmol of octanoic acid. (b) 2.5 mmol of octanoic acid. (c) 1 mmol of octanoic acid and 1 mmol of bis(2-ethylhexyl)amine. (d) 1 mmol of bis(2-ethylhexyl)amine. (e) 2.5 mmol of bis(2-ethylhexyl)amine. The scale bars in all the figures are 100 nm.

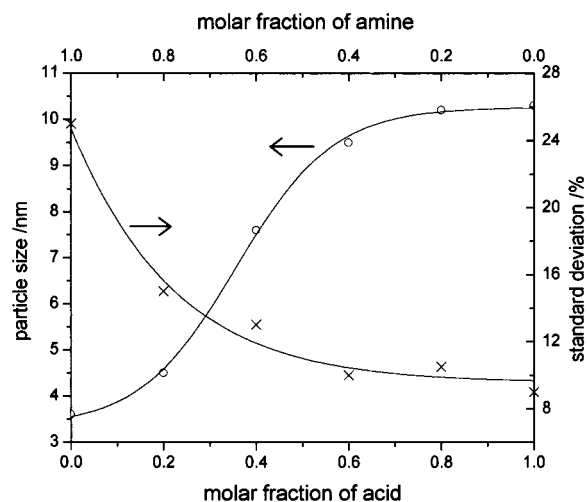
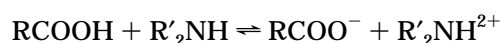


Figure 2. Effect of the composition of the protective agent on the size and size distribution of the resultant nanoparticles.

solutions of nitrogen nucleophiles, carbonyl groups in $\text{Fe}(\text{CO})_5$ were partially replaced, forming metal cluster compounds more thermally labile than $\text{Fe}(\text{CO})_5$.¹² Therefore, a higher concentration of amines in the system should accelerate the decomposition of $\text{Fe}(\text{CO})_5$ and higher reaction speed would favor spontaneous nucleation of the metal nanoparticles; thus, more nuclei would be generated in the system, which results in smaller but nonuniform nanoparticles.

Because the major goal of our research is to prepare small and uniform nanoparticles with control of the sizes, we decided to test the effect of using mixed long-chain acid and long-chain amine as protective agents. Figure 1C shows nanoparticles using a mixture of 1.0 mmol of bis-2-ethylhexylamine and 1.0 mmol of octanoic acid as protective agents. The size of Fe–Mo nanoparticles was reduced to 4.2 nm with an even narrower size distribution than nanoparticles prepared using octanoic acid alone. The improvement in both the size and distribution using mixed protective agent is a strong indication that a carboxylic acid and amine mixture can act as a more efficient protective agent than carboxylic acid alone.

We believe such an improvement in the protecting ability for the mixture of acid and amine is due to the formation of carboxylate anions. Normally, the carboxylic acid molecules are present as dimers in nonpolar solvents because of the hydrogen-bonding interaction. The electron-donating ability of the oxygen atoms in the molecules is reduced due to H-bonding. But when amine is added to the system, the carboxylic acid molecules are partially transformed into carboxylate anions according to the following equilibrium:



It is known that the carboxylate anions have a higher electron-donating ability. Therefore, they interact with

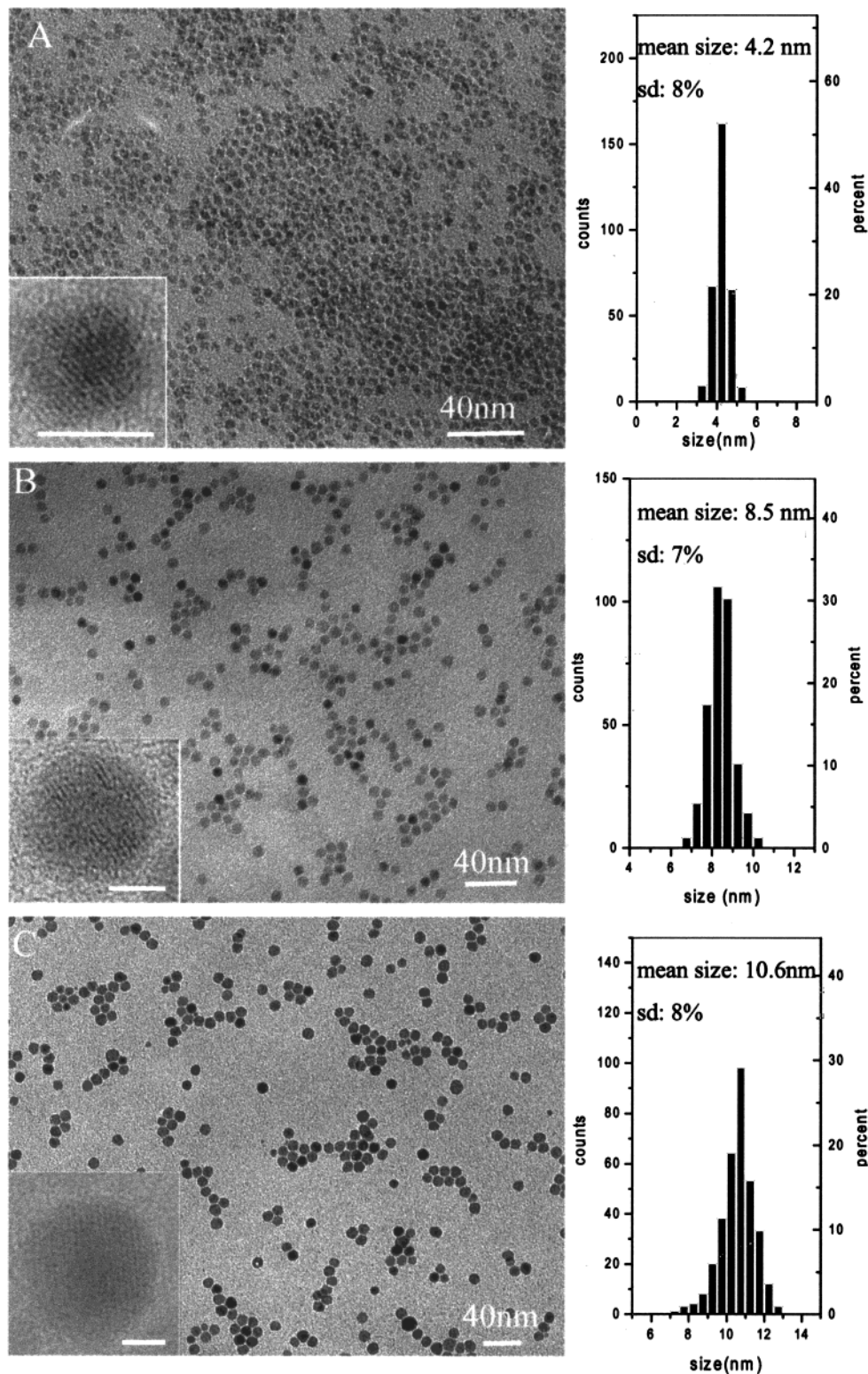


Figure 3. TEM images of Fe–Mo nanoparticles synthesized under typical conditions (a) and 2.50 mmol (b) or 5.00 mmol (c) of protective agent was used. The scale bars in the inserts are all 4 nm.

the nanoparticles more strongly and the nanoparticles are protected more efficiently. The FTIR spectra of the 1:1 mixture of octanoic acid and bis-2-ethylhexylamine in octyl ether shows a band at 1556 cm^{-1} , clearly indicating the formation of carboxylate anions in the mixture.

We have also found that both the molar ratio between acid and amine and the total concentration are very

important factors that affect the final size and distribution of the nanoparticles. Figure 2 shows the effect of the acid/amine ratio on the final size of nanoparticles when the total concentration of acid and amine is fixed at 2.5 mmol. It shows that the more acid used in the mixture, the bigger the nanoparticles. However, the uniformity of the nanoparticles improves significantly with an increasing amount of acid. So to prepare small

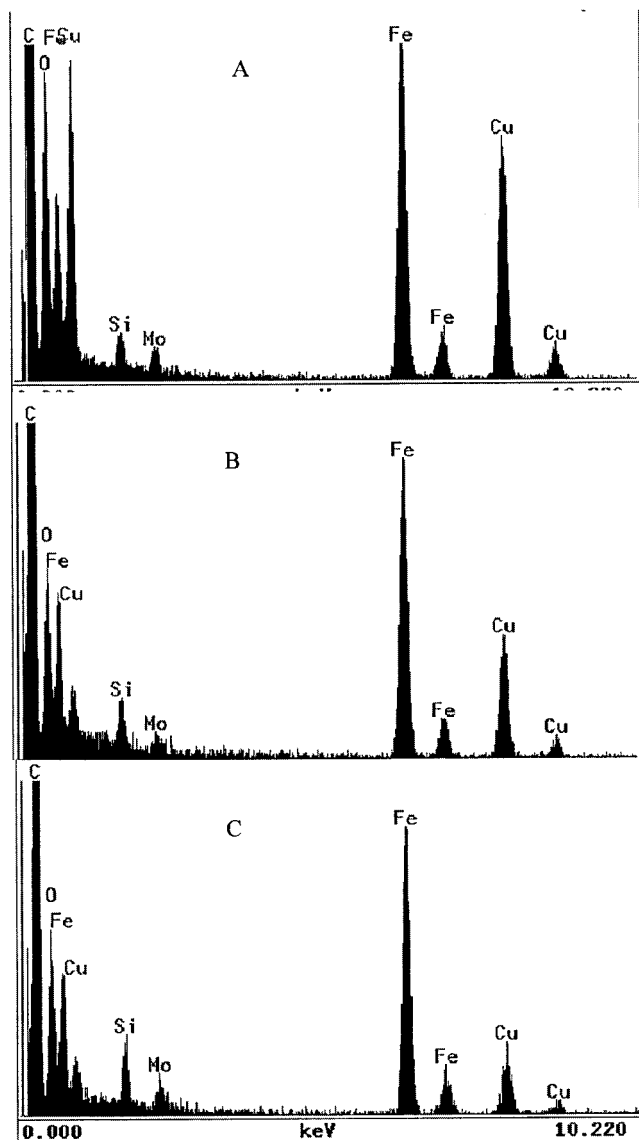


Figure 4. EDX spectra of the nanoparticles shown in Figure 3.

but uniform nanoparticles, we chose a mixture of octanoic acid and bis-2-ethylhexylamine with a 1:1 mole ratio as the protective agent in our experiment.

Size Control. Using a 1:1 mixture of bis-2-ethylhexylamine and octanoic acid, we have prepared uniform Fe/Mo nanoparticles with control over their sizes by varying the experimental conditions. Figure 3 shows the TEM images of three samples with the average sizes of 4.2, 8.5, and 10.6 nm, respectively. Over 300 particles were measured for each sample to get the size distributions shown in Figure 3. The standard deviations of these samples are all <8%. The HRTEM images show that the particles have a highly crystallized structure. The EDX spectra (Figure 4) show that all the samples have the composition of 96 wt % (98 mol %) of iron and 4 wt % (2 mol %) of molybdenum. The products contain less molybdenum than the initial reactants. This may be caused by the slower decomposition rate of $\text{Mo}(\text{CO})_6$ under the reaction conditions.

We have investigated the dependence of the particle size on the reactant concentration, reaction time, and molar ratio of metal carbonyl and protective agents. As

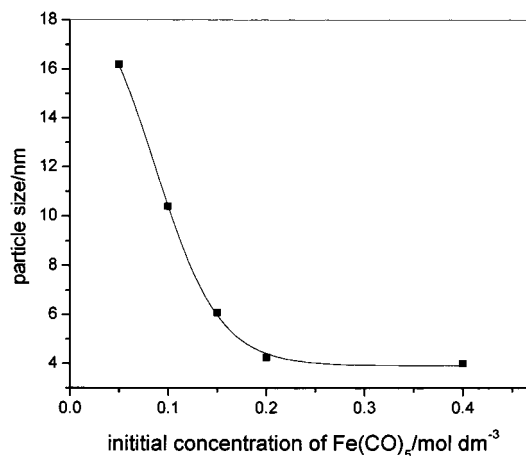


Figure 5. Effect of the initial reactant concentration on size of the resultant nanoparticles.

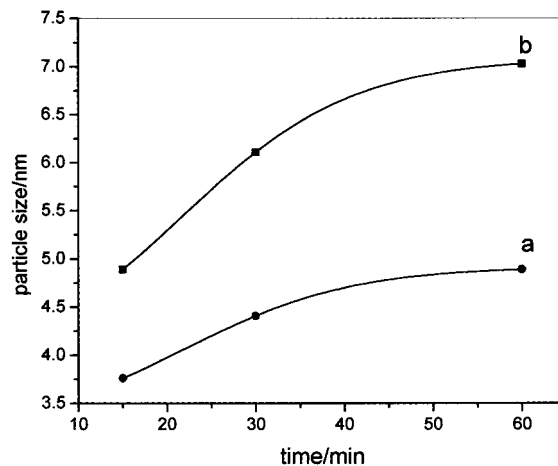


Figure 6. Time dependence of the particle size. (a) 1.00 mmol of protective agent was used. (b) 2.00 mmol of protective agent was used.

shown in Figure 5, we have found that when the molar ratio between the protective agent and the initial reactants $\text{Fe}(\text{CO})_5$ was fixed to 1, the size of the nanoparticles increases when the reactant concentration decreases. At extremely low concentrations, the particle size decreases sharply with an increase in the initial reactant concentration; after that, the particle size only has a very small change with the change of reactant concentration. In such a complex system, the size of the produced nanoparticles depends on many factors, including the number of nuclei created, the total concentration of reactants, and the effect of protective agents. This observation indicates that the nucleation step is the dominating factor that determines the final size of the particles at lower concentration. It suggests that the number of nuclei decreases as the total concentration of reactant decreases, and a smaller number of nuclei makes larger particles.

Figure 6. shows that the particles grow larger with the reaction time at shorter reaction times and then stop growing when the reaction time approaches 60 min. Presumably, all the metal carbonyl molecules are consumed at that stage.

We also found that the molar ratio between the protective agents and the reactants is an extremely important factor that determines the particles' size. The

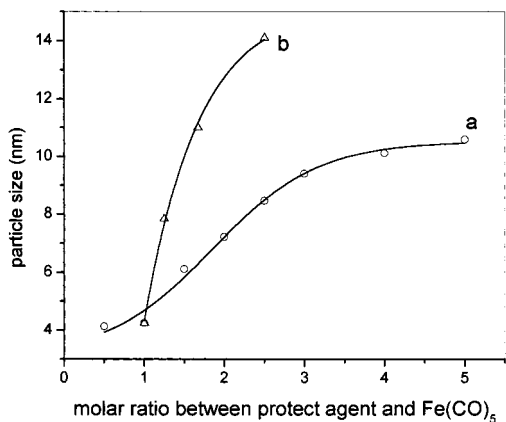


Figure 7. Effect of the molar ratio between protective agent and $\text{Fe}(\text{CO})_5$. (a) The initial amount of $\text{Fe}(\text{CO})_5$ was fixed at 1.00 mmol, and the amount of protective agent varied. (b) The amount of protective agent was fixed at 1.00 mmol and the amount of $\text{Fe}(\text{CO})_5$ was changed.

results were shown in Figure 7. Here, the molar ratio refers to the ratio between octanoic acid (equal amount of bis-2-ethylhexylamine is also added at the same time) and $\text{Fe}(\text{CO})_5$. The experiments were performed in two ways: one, by fixing the initial concentration of the reactants and changing that of the protective agent, and two, by fixing the concentration of the protective agent and changing that of the reactant. Both show that the particles become larger when the molar ratio between the protective agent and the reactants increases. Because of the concentration effect, the slope of curve (b) in Figure 7 is much larger than that of (a). The increase of the particle size with the increasing amount of the protective agents is very surprising. It is generally believed that as the amount of protective agents increases, the particles are protected more thoroughly immediately after their formation; therefore, they should become smaller. One possible explanation is that the protective agents used in the experiment may have a strong effect on the decomposition speed of the metal carbonyl. The evidence we have is that as the amount of protective agents increases, the time it takes for the reaction mixture to turn black (as an indication of the formation of metal nanoparticles) increases from ~ 3 to ~ 20 min. Because slower reaction speed normally means a smaller number of nuclei are formed initially, bigger nanoparticles are thus produced. The same effect was also observed when only acid was used. This shows that the possible candidates that reduce the decomposition speed of the metal carbonyl compounds are carboxylic acid molecules and/or carboxylate anions. To make things more complicated, the reverse trend in the decomposition speed was observed when pure bis-2-ethylhexylamine was used as the protective agent as discussed in an earlier section, indicating that amine could accelerate the decomposition. When the acid/amine mixture was used, clearly the effect of the acids and carboxylates that stabilized the metal carbonyls was the dominating effect, as indicated by our observation. More work is needed to fully understand the mechanism of the reactions and the effect of different parameters in such a complicated system. Nevertheless, we are able to prepare uniform Fe/Mo nanoparticles with controllable sizes by varying the experimental conditions.

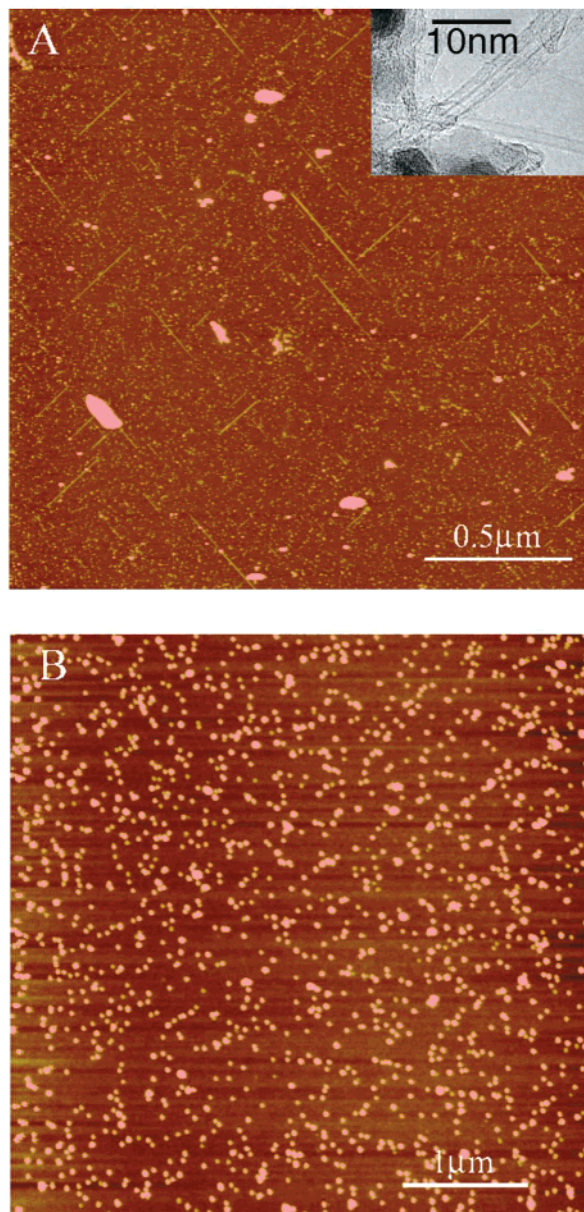


Figure 8. AFM images of the $\text{Al}_2\text{O}_3/\text{Si}$ wafers with 3.6 nm (a) and 8.5 nm (b) Fe–Mo nanoparticles on the surface after the CVD process. The insert in (a) shows TEM images of nanotubes grown with 3.6 nm nanoparticles supported on fumed alumina powder under the same growth conditions.

Nanotube Synthesis. We have grown single-walled nanotubes on Al_2O_3 surfaces with the synthesized Fe–Mo nanoparticles as the catalysts using our previously reported procedure.²⁰ We have found that the initial size of the catalyst particles is an important factor for the nanotube growth. As shown in Figure 8, large numbers of nanotubes were found in the sample when Fe/Mo nanoparticles of 3.6 nm were used as the catalyst, but no tubes were observed in the samples with 8.5 nm nanoparticles as the catalyst. The TEM image in the figure shows that the nanotubes grown under our experimental conditions are single-walled nanotubes. This indicates that there is an upper limit for the size of the catalyst particle to nucleate single-walled carbon nanotubes and this limit is between 4 and 8 nm under our growth conditions. More systematic studies of the relation between the size of the particles and the

diameter of the produced tubes for both single-walled and multiwalled nanotubes are underway in our group.

In summary, we have discovered a solution-based method for the preparation of uniform Fe-containing metal nanoparticles. The sizes of the produced nanoparticles can be varied systematically between 3 and 14 nm by changing the experimental conditions. The produced nanoparticles have been used as catalysts for carbon nanotube growth and the experimental results indicate that there is an upper limit for the size of the

catalyst particle to nucleate a single-walled carbon nanotube.

Acknowledgment. This work is in part supported by the start-up fund from Duke University and by a Multidisciplinary Research Program of the University Research Initiative (MURI) from the Office of Naval Research Grant 00014-98-1-0597 through UNC-CH.

CM000787S